8

Analyzing DNA Structure Quantitatively at a Single-Molecule Level by Atomic Force Microscopy

Yong Jiang and Yuan Yin
School of Chemistry and Chemical Engineering, Southeast University, Nanjing P. R. China

1. Introduction

The atomic force microscope (AFM), one of the most popular types of scanning probe microscopy, was invented by Binnig *et al* [1] in 1986. After that, its quick development resulted in the commercial AFM available at 1989 to the biological and chemical researchers. Two decades after its invention, now it has become a standard measurement technique in multiple branches of science and technology. The AFM's advantage over other techniques stems from its ability to work in different environment. It can work in vacuum, liquid, or ambient, and in addition its high resolution and sensitivity to measure spatial sizes and forces, respectively. The technique thus not only provides sharp images of nonconductive surfaces at a resolution of nanometer scale, but also enables the measurements of intra- or inter-molecular forces at a resolution of pico-newton scale. These properties make AFM ideal for biological samples, especially for DNA molecules.

The schematic in Figure 1A illustrates the basic principles of the AFM operation. A sharp tip reads the profile of the sample by scanning the surface. The tip is attached to a cantilever that works as a spring pressing the tip against the sample. The vertical position of the tip is measured by a laser reflected from the cantilever to the position of sensitive photo detector (PSPD). Three important features of the AFM instrument are listed below. First, the position of the sample relative to the tip is controlled by the scanner and it can be done with accuracy better than 1 nm. Second, the tip may be made tremendously sharp or customized for the desired measurement. Third, the vertical displacement of the tip relative to the surface is determined with sub-nanometer precision. These three major features allow AFM to provide the topographic image with nanometer resolution.

Figure 1B illustrates the major operation modes of the AFM. The manner of the microscope operation corresponding to the attraction part of the tip-sample interaction potential is non-contact mode (NC-AFM) [3]. A breakthrough in the high-resolution AFM imaging was made with implementation of the NC-AFM mode, offering a unique tool for real space atomic-scale studies of surfaces and nanoparticles. The probe of NC mode does not contact the sample surface, but oscillates above the adsorbed fluid layer on the surface during scanning. Using a feedback loop to monitor changes in the amplitude due to attractive forces the surface topography can be measured. After tip-surface attraction force passes the minimum

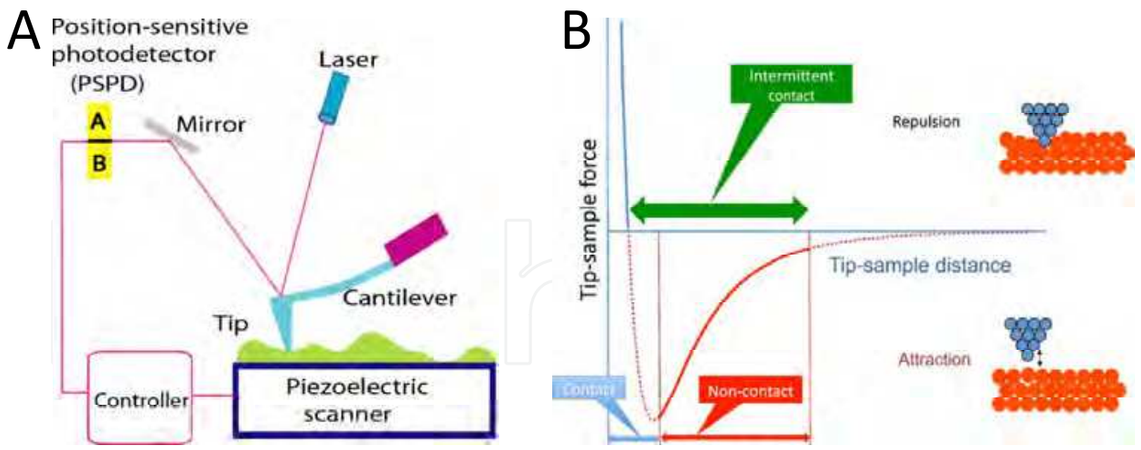

Fig. 1. (A) Schematic explaining the principles of AFM operation. The position of the tip relative to the sample is controlled by a piezoelectric scanner. The vertical displacement of the tip during scanning is detected using the optical lever principle, in which the position of the light spot on the position of sensitive photo detector (PSPD) is measured. (B) Scheme explains the operation modes of the AFM. A curve in the scheme shows the change of the tip-sample interaction depending on the distance between the apex of the tip and the sample. (Adapted and modified from reference [2], with permission)

on the potential curve, the repulsion interaction increases very fast, achieving large positive values in the very short range of the tip-sample distances. This scanning way is called contact mode. Since the interaction of the tip and the surface is so strong, the deformation of a soft sample typically occurs, and as the results of it, the soft sample may be damaged or moved by the sharp tip. Schematically, this deformation is occurred in the top right cartoon by displacement of the red spheres [3]. For hard samples at small tip-surface separation, the pressure created by the tip at the apex is so large that atoms can jump from tip to surface and vice versa. Therefore, contact mode of the AFM operation does not obtain reliable and stable images at atomic resolution for both soft and hard sample. In addition, damage or movement of soft biological samples can be made to the tip during approach or scanning process. Tapping modes with small pressure can obtain reliable and stable images at atomic resolution for any samples. The imaging of tapping Mode is alike to contact mode. However, in this mode the cantilever is oscillated at its resonant frequency. The probe lightly "taps" on the sample surface during scanning, contacting the surface at the bottom of its swing. By maintaining constant oscillation amplitude, a constant tip-sample interaction is maintained and an image of the surface is obtained. Tapping mode allows high resolution of samples that are easily damaged or loosely held to a surface, especially good for biological samples. As a summary, non-contact and tapping modes are two optional modes for DNA imaging.

Since the AFM physically interacts with the sample, the AFM can work as a force spectroscopy by stretching a single molecule between the tip and sample surface. If the spring constant of the cantilever is obtained, the AFM is an excellent force spectroscopy for probing the mechanical properties of individual molecules because it can measure their length and tension with nanometer (nM) and piconewton (pN) resolution, respectively. The working principle of an AFM force spectroscopy is shown in Figure 2. A laser is reflected

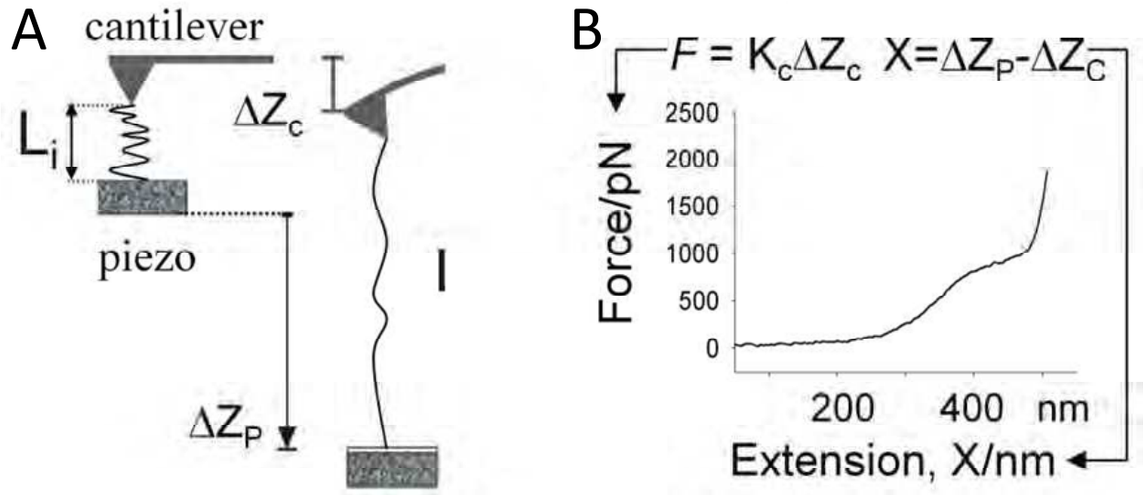

Fig. 2. AFM force spectroscopy: (A) Diagram of a single stretching experiment; (B) Example of a force extension curve, with definitions of force and extension. (Adapted and modified from reference [4], with permission)

off the back of the cantilever onto the center of the PSPD. The sample is fixed on the piezoelectric positioner and the molecules on the sample can attach to the tip by moving up the sample to physical contact it. The molecules are normally connected on the substrate or tip by nonspecific adsorption or designed chemical bond. In this way, the molecules form bridges between the substrate and the tip (Figure 2A). These molecules can be stretched and relaxed in a controlled manner by moving the substrate away and back from the tip. The stretched molecule exerts a mechanical force on the cantilever, thereby deflecting it. Because the force applied is much smaller than the chemical bond between the molecule and substrate or tip, the molecule will not detached from the substrate or tip during repeated stretching. This deflection is measured by the photodiode as a change in the voltage generated by the movement of the incident laser beam off of the photodiode center. The experimental result is a force-distance curve (force spectrogram) that reflects the elasticity of a single molecule, which for example was shown in Figure 2B.

In the last decade, AFM has proven to be one of most valuable techniques for the studies of DNA and the researches were mostly focused on the biological structure and dynamic processes of DNA [5-10]. However, AFM is normally used to gain qualitative results at a single-molecular level. By analyzing the topological structure of each DNA molecule from AFM images, the distributions of DNA with different configurations can be identified directly and easily. Due to this advantage, AFM imaging can also be ideal tool for quantifying DNA structure under a wide range of DNA amounts, concentrations and sizes that may not able to be handled by other methods. It has been demonstrated that AFM is capable of quantifying DNA plasmids with the amount less than 1 pico gram and the size up to 100 kilo base pairs. However, the application of AFM techniques in quantitative research is limited because of the lack of comparative studies with other traditional and well-established methods, such as gel electrophoresis. After we compared the results obtained by AFM with that obtained by gel electrophoresis [11-14], AFM was proven to be an accurate method in the identification and quantification of the DNA with different

topological structures. Therefore, the purpose of this chapter is to present this single-molecule AFM imaging and force spectroscopy techniques that we developed for sensitive and quantitative analysis of DNA structure. We believe that this chapter will help to expand the application of AFM techniques in DNA research.

2. Materials and methods

2.1 Materials

pUC18, 2686 base pairs (bp), was isolated from *E. coli* and purified using the QIAFILTER plasmid maxi kit (QIAGEN Inc). pNEBR-R1 was purchased from New England Biolabs (Beverly, MA). Single-stranded poly(dA) was purchased from Sigma-Aldrich, Inc. (St. Louis, MO).

2.2 Sample preparation

For experiments in which the imaging buffer contains Mg^{2+}, freshly cleaved mica was used as DNA substrate directly. For experiments in which the imaging buffer did not have Mg^{2+}, 1-(3-Aminopropyl)-silatrane functionalyzed mica (APS-mica) was used for the binding of DNA molecules. APS-mica was prepared as described by Shlyakhtenko et al [15]. A drop of 10-50 µl of DNA solution (0.5-1 µg/ml) was deposited on the APS-mica surface at room temperature for 3 min. The sample was rinsed and air-dried before imaging. For AFM force spectroscopy, 80 µl of DNA solution (~60 ng/µl) in Tris-EDTA buffer (10 mM Tris+HCl, 1 mM EDTA, pH 8; Sigma-Aldrich, Inc), supplemented with 150 mM NaCl, was deposited onto a freshly evaporated gold surface. After the sample was incubated for 2-3 hours, it was gently rinsed 3-5 times with the buffer solution before test.

2.3 AFM imaging

AFM topographic images were taken using a Nanoscope IIIa MultiMode Scanning Probe Microscope (Veeco Instruments Inc) using Tapping mode with an E scanner. RTESP probes (Veeco) were used for imaging in air. The spring constant of AFM cantilevers was 20-80 N/m and their resonance frequency was 275-316 kHz. NP-S probes (Cantilever C) were used for imaging in solution. The spring constant of the cantilever was 0.32-0.64 N/m and their resonance frequency was 56-75 kHz. All of the images were collected at a scan rate of 2-3 Hz, a scan resolution of 512×512 pixels, and scan sizes of 1-5 µm.

2.4 Quantifying DNA structures from AFM images

The number of DNA with different configurations i.e. the damage, was quantified by a Poisson distribution $f(n; \lambda)= \lambda^n \times exp(-\lambda)/n!$ [16,17], based on percentages of supercoiled and relaxed DNA. The average number of damage per molecule, λ, can be obtained from $\lambda=-ln[f(\lambda; 0)]$, where $f(\lambda; 0)$ is the fraction of supercoiled (damage n=0) plasmids.

2.5 AFM force spectroscopy

For force spectroscopy measurements, we used nonspecific adsorption of DNA to fresh gold substrates [18] and untreated silicon nitride AFM probes (MLCT from Veeco). The cantilevers had a nominal spring constant of 10 mN/m and an actual spring constant between 10-20

mN/m, as determined by using the energy equipartition theorem [19]. 80 µl of ssDNA solution (~60 ng/µl) in Tris-EDTA buffer (10 mM Tris+HCl, 1 mM EDTA, pH 8; Sigma-Aldrich, Inc), supplemented with 150 mM NaCl, was deposited onto a freshly evaporated gold surface. After the sample was incubated for 2-3 hours, it was gently rinsed 3-5 times with the buffer solution.

3. Results and discussion

3.1 Analyzing DNA structure quantitatively at a single-molecule level by AFM

Plasmid DNA is broadly used as a model in DNA research because it has three different conformations: supercoiled forms, relaxed forms, and linear forms depending on structural modification such as single strand breaks (SSB) or double strand breaks (DSB) [11,20,21]. It is because intact plasmid DNA will relax to open circular form even though one SSB is introduced. Likewise, the ring-shaped plasmid will open and change to linear form if one double strand break takes place and more DSBs will fragment the plasmid to linear segments of shorter lengths. All these topological/lengths transformation of DNA are easy to resolve and quantify by gel electrophoresis [22-24] and AFM [7,8,25-29]. However, it is very important to know that some structural changes may occur in intact supercoiled DNA upon the binding of plasmids to the mica surface. This problem has been solved by Shlyakhtenko et al. who used APS-mica [15,30] instead of fresh-cleaved mica. The results revealed that the conformation of supercoiled DNA remains practically unchanged when DNA binds from high salt buffer solutions to the APS-mica. Unlike untreated mica, which is negatively charged and therefore demands a high concentration of divalent cations and a relatively low concentration of monovalent cations for a deposition of DNA, APS mica is positively charged and supercoiled DNA becomes immobilized quite effectively in the presence of high monovalent salts, and as a result, the topology of the DNA will not be affected.

A typical AFM image, shown in Figure 3A, presents the plectonemic supercoiled configuration of pUC18 molecules after they had been deposited on the APS-mica. Following methods developed earlier for electron microscopy and AFM imaging of supercoiled plasmids [20,26,31], the number of nodes, generated at visible crossover points (figure 3A), was counted within single DNA molecules, and the distribution of the number of nodes was shown in Figure 3B. For a given plasmid size, the number of supercoiled nodes typically follows Gaussian distribution and also shifts according to the type and the concentration of cation and deposition conditions [32]. In the case of pUC18, the same buffer with 100 mM NaCl was employed in all experiments, so this error can be eliminated. For intact pUC18, the average number of nodes is eight, and this is consistent with the previously reported value for a supercoiled DNA composed of 2686 base pairs [20,21,26,33]. 5% of the plasmids show fewer than six nodes, which might imply that these plasmids represent a background of damaged DNA in our sample after extraction and purification using the QiaFilter plasmid maxi kit. Further experiments, using T4 Endonuclease V to nick pUC18 plasmids which were exposed to UV radiation, support our criterion of five nodes as the borderline between damaged and undamaged DNA. In the following discussion, we suppose that pUC18 molecules with a number of nodes greater than five are intact, while the number of nodes equal to or less than five will be indicative of some structural alterations within supercoiled DNA. Based on this assumption, our pUC18 DNA samples have 95% of intact supercoiled DNA.

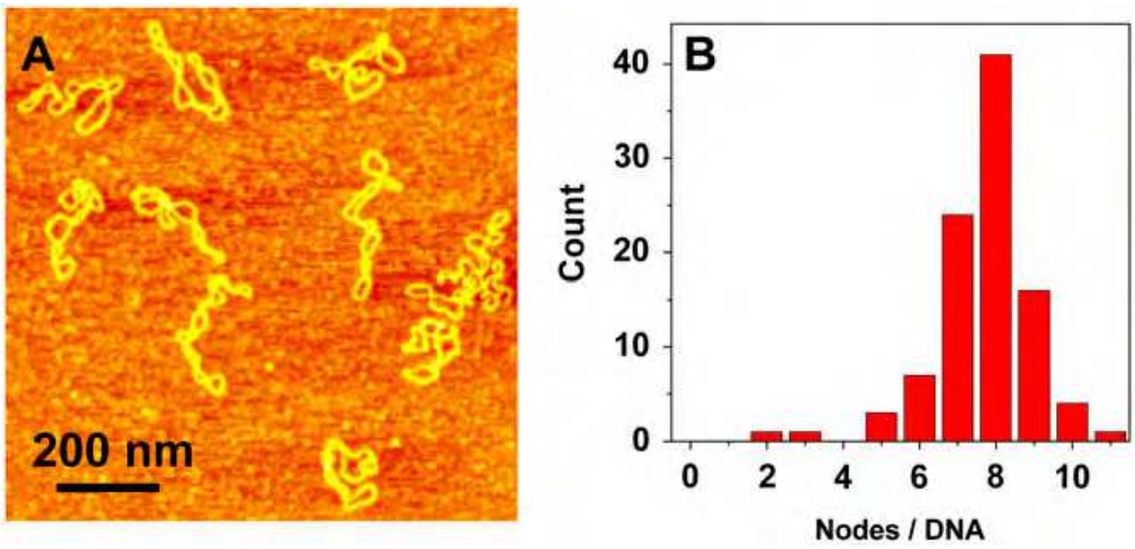

Fig. 3. (A) An tapping-mode AFM image of intact pUC18 plasmids adsorbed to APS-mica surface reveal their supercoiled topology. AFM was performed in tapping mode at a scan size 1×1 μm². (B) The frequency distribution of the number of supercoiled nodes in intact pUC18 plasmids (based on 21 AFM images). (Adapted and modified from reference [11], with permission)

Figure 4 shows the AFM images of pUC18 molecules exposed to UVB (302 nm) radiation. From Figure 4A and D, we discover that at a dose of 1.4 kJ/m², the configuration of DNA molecules did not change obviously as compared to the intact molecules shown in Figure 3A and B, with 95% of the plasmids having more than five supercoiled nodes. 5% of the plasmids have five or fewer nodes, which represent a background damage of our pUC18 DNA. In Figure 4B and C, pUC18 molecules were exposed to 165 kJ/m² and 660 kJ/m² of UVB radiation, respectively. Among molecules subjected to 165 kJ/m², 78%± 1% are relaxed circular plasmids and 16% are linear fragments (Figure 4B and E). At 660 kJ/m² of UVB radiation, this fraction, including fragments with an obviously reduced length, increased to 91% (Figure 4C and F). Therefore, our results suggest that UVB can cause significant degradation of DNA. The results of the three tests are graphically summarized in Figure 4 G.

One SSB is enough to relax a whole supercoiled plasmid, and the increasing size of the plasmid also increase our measurement sensitivity. To check this assumption, a bigger plasmid named pNEBR-R1 supercoiled DNA (10,338 bp) was irradiated with 29 J/m² of UVB and treated with T4 Endonuclease V. Figure 5 display a representative AFM image of these plasmids. 55% of pNEBR-R1 plasmids are in the relaxed circular form and 14% are in the linear form counted from similar images. In control experiments on pUC18 molecules, the percentages of supercoiled, relaxed circular and the linear form of DNA are 65%, 34% and 2%, respectively. From the percentage of supercoiled molecules, we evaluate that pNEBR-R1 plasmids contained 1.12 CPD/plasmid (λ=1.12), while for pUC18, the average number of CPD lesions per DNA plasmids is 0.4 (λ=0.4). So, increasing the size of the supercoiled plasmid by 3.8 fold (10338/2686) lead to a 2.8 fold (1.12/0.4) increase in damage detection sensitivity, which is consistent with our predictions.

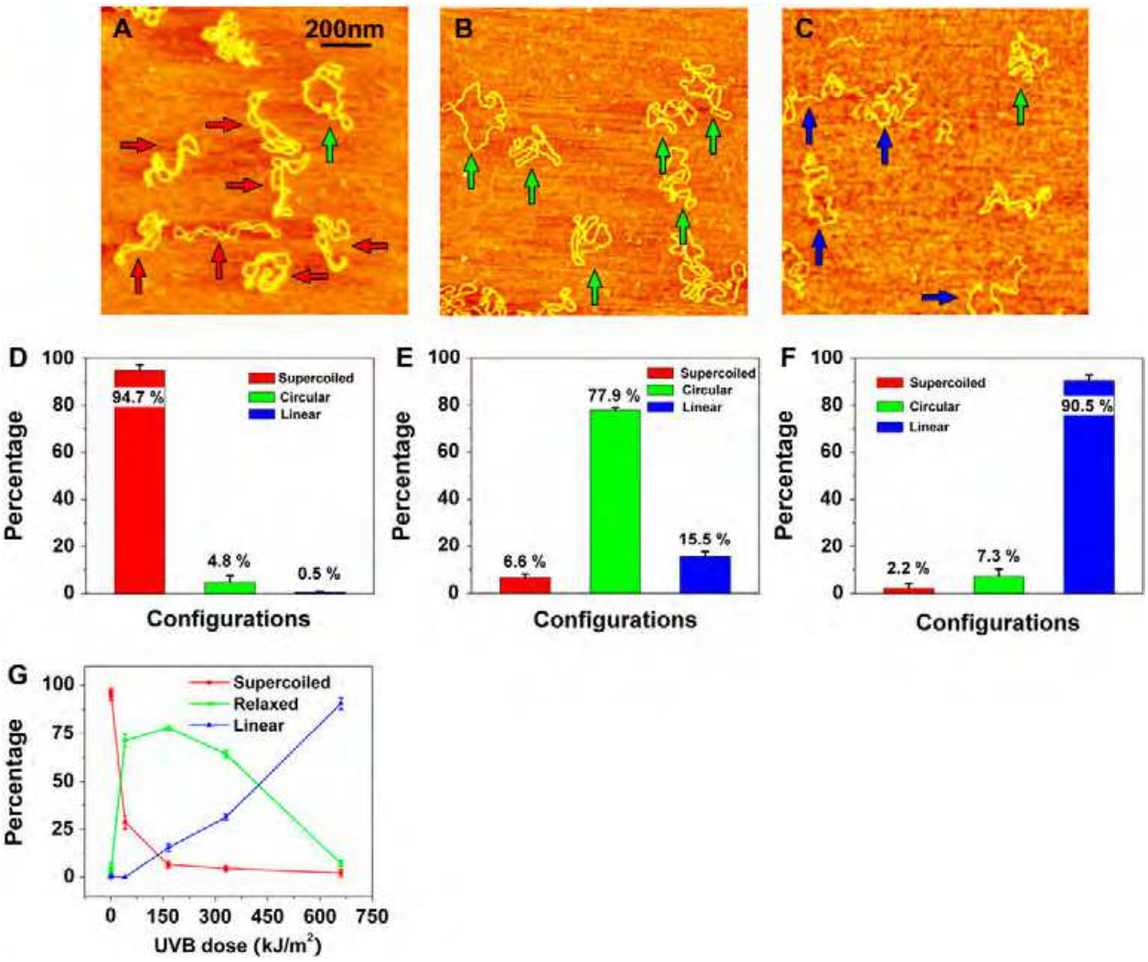

Fig. 4. AFM images of pUC18 molecules subjected to different doses of UVB radiation: (A) 1.4 kJ/m², (B) 165 kJ/m², (C) 660 kJ/m². Scan size in all the images is 1×1 μm². (D–F) Histograms of the occurrence of various configurations of pUC18 plasmids determined from the AFM images such as these shown in (A–C). (G) Percentages of different configurations of irradiated pUC18 as a function of UVB dose. Color code for the arrows, histogram and curves: red, supercoiled DNA; green, relaxed circular plasmids; blue, linear DNA. (Adapted and modified from reference [11], with permission)

Agarose gel electrophoresis is an extremely powerful, versatile, easy to use, sensitive, and quite rapid technique for quantitative DNA research, and contributed enormously to the progress of DNA damage and repair research. The three unique features of AFM that make it particularly suitable for quantitative DNA studies are a), the ability to examine individual DNA molecules and DNA protein complexes, b) molecules can be investigated under nearly in vivo conditions, and c), extremely small amounts of DNA and protein material are needed for the observation. To demonstrate this last point, 0.1 ml of a pUC18 plasmid solution containing the total amount of 1 pg of DNA (10 pg/ml) was coated over the mica surface and imaged at a scan size (5×5 μm²). The AFM image, shown in Figure 6, captured four individual DNA molecules whose configuration was evaluated by scanning locally at a higher resolution. Thus, the amount of DNA need for this measurement is ~400 times less

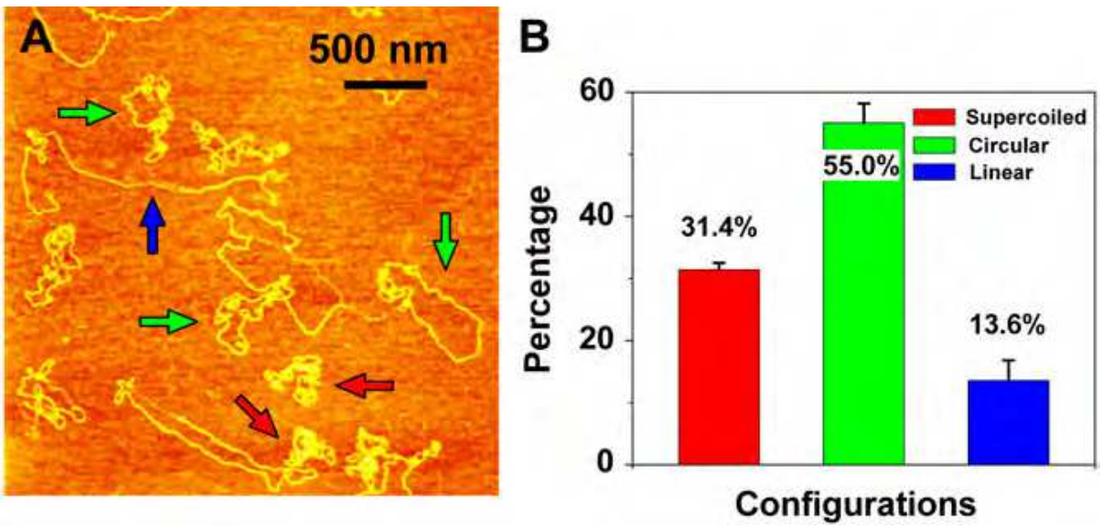

Fig. 5. Sensitivity of damage detection increases with plasmid size. (A) An AFM image of supercoiled plasmid pNEBR-R1 (10,338 base pairs) irradiated at 29 J/m² UVB. Scan size 3×3 μm². (B) Percentages of different configurations of pNEBR-R1 plasmids determined from AFM images such as these shown in A. (Adapted and modified from reference [11], with permission)

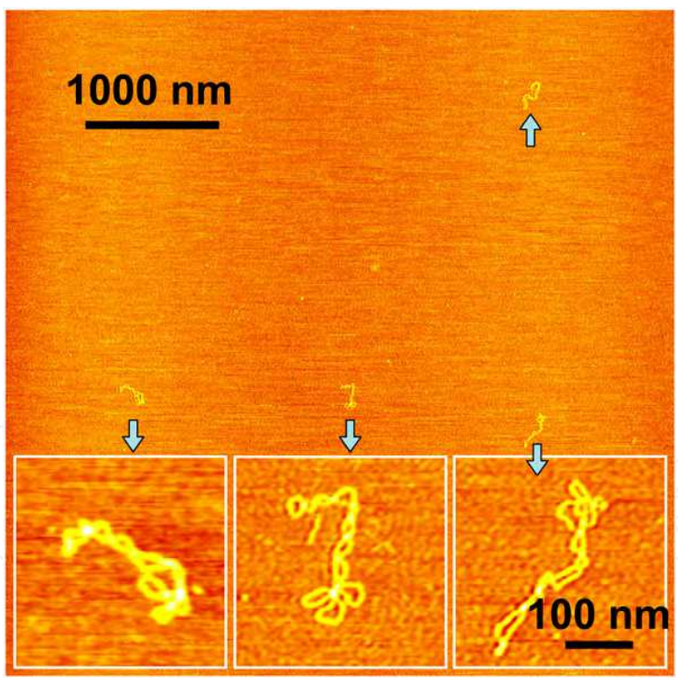

Fig. 6. An AFM image of intact pUC18 plasmids obtained from a sample that contained a total amount of 1 pg of DNA material. Scan size is 5×5 μm². The inset images obtained at a higher resolution show in detail the supercoiled structure of these plasmids. The scale bar for these inset images is 100 nm. The sample was prepared by spreading 0.1 ml of a 10 pg/ml solution of pUC18 on the APS-mica surface and incubating for 3 min. This assay requires extremely small amounts of DNA to evaluate damage. (Adapted and modified from reference [11], with permission)

than what is needed for the most sensitive gel electrophoresis assays presently [34], which amounts to ~1/5 of the DNA in a single cell. In some studies, it may be very useful to combine the advantages of gel electrophoresis with AFM imaging. Gel electrophoresis would separate the DNA into discrete bands, and the DNA extracted from a particular band would provide enough material for further examination by high resolution AFM imaging. It has been demonstrated that AFM is capable of quantifying DNA plasmids smaller than 100 kilo base pairs and total mass smaller than 1 pico-gram.

3.2 AFM method for DNA quantification is consistent with gel electrophoresis

Before comparing the accuracy of AFM imaging with gel electrophoresis, we need to calibrate both methods by working on a mixture with known composition. A mixture of supercoiled and linear pUC18 with a ratio of 1:1 was used as the reference sample, and was deposited on APS-mica for AFM imaging. From the image in Figure 7A, we can identify both supercoiled and linear forms clearly. Intact plasmid (labeled by letter "S") has a supercoiled configuration, while linear DNA (labeled by letter "L") has two clear ends. By counting the numbers of DNA in different structures in this image and different images on the same sample, the actual ratio of supercoiled and linear DNA on the mica surface was acquired. The result is summarized in Table 1. Supercoiled and linear DNA percentages were 50.1% and 48.1%, respectively, a ratio of linear/supercoiled DNA of 0.96 (the true value is 1 here). This means that the error is quite small, with no necessary calibration. It also means that the topological structures cannot be affected by DNA binding to mica during the sample preparation and AFM scanning process by sharp tips.

The ratio of different conformations (supercoiled, relaxed or linear forms) can be inferred to the numbers of SSB and DSB, which represent the level of DNA damage [15,17]. However, these three forms have the same sequence (molecular weight), so it is difficult to separate them by normal methods. Gel electrophoresis is one of the well-established methods to separate them since different topological structures have different radii of gyration and electrophoretic nobilities. DNA mobility of supercoiled DNA is much greater than that of its relaxed circular form. Therefore, it is significant to compare our results obtain by AFM imaging with the results obtained by gel electrophoresis assay.

We made the gel electrophoresis assay on the same DNA sample as used for AFM imaging. The relative amounts of DNA in various bands were quantified by measuring the intensities of each band in the gel photo. The gel is shown in Figure 7B and the results are summarized in Table 1, indicate a nonlinear relationship between the relative amounts and the band intensities of DNA in supercoiled forms versus linear forms. Supercoiled DNA is less fluorescent compared with circular and linear forms [20,30]. Therefore, quantification of supercoiled DNA by band intensity is much more complicated, compared to that of relaxed forms or linear forms.

In order to further test whether AFM imaging is an accurate method for DNA quantification with various topological configurations, the same DNA sample extracted from an agarose gel was used for AFM imaging. A mixture of supercoiled and relaxed pUC18 plasmids was chosen as model DNA. After the mixture was loaded on a gel electrophoresis, two bands which contain supercoiled DNA and relaxed DNA were separated as shown in Figure 8A. The DNA molecules in the supercoiled and relaxed DNA gel bands were extracted and purified back into solution separately for further AFM imaging. Figure 8B and C show the

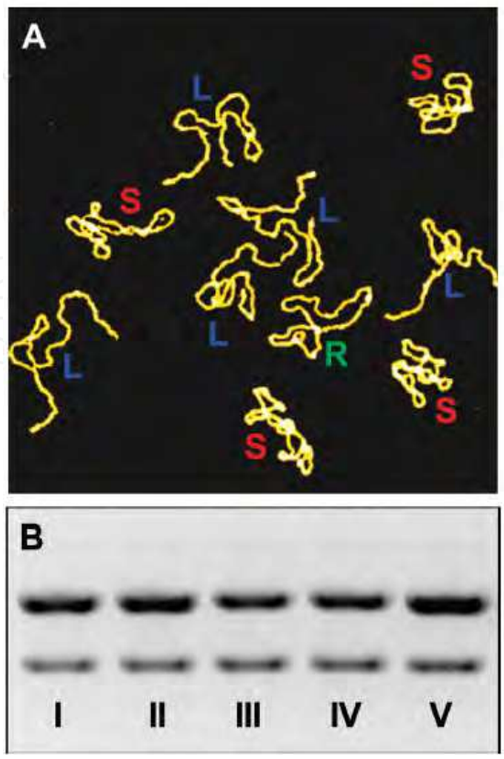

Fig. 7. (A) An AFM image showing the mixture of supercoiled and linear pUC18 DNA with the same weight ratio. Scan size is 1 × 1 μm². Color code: red, supercoiled DNA (S); green, relaxed circular plasmids (R); blue, linear DNA (L). (B) A photograph of the agarose gel showing the separated supercoiled and linear pUC18 bands on the same sample as shown in part A, with the same weight ratio. The gel was run with (I) *E. coli* Endonuclease IV reaction buffer, (II) *E. coli* Endonuclease IV enzyme and its reaction buffer, (III) *E. coli* Endonuclease V reaction buffer, (IV) *E. coli* Endonuclease V enzyme and its reaction buffer, (V) 10 mM Tris-HCl, 1 mM EDTA, and 100 mM NaCl buffer. The top bands in all lanes contain linear pUC18 while the bottom bands represent supercoiled DNA. The image was treated with flatten function in operation software (Veeco Inc.) to get rid of the background noise. (Adapted and modified from reference [13], with permission)

Band intensity	AFM	GEL		
		Tris, EDTA & NaCl	Endo-IV enzyme and its buffer	Endo-V enzyme and its buffer
Supercoiled%	50.1	32.6	32.2	38.4
Relaxed%	1.8	x	x	x
Linear%	48.1	67.4	67.8	61.6
Correction factor	0.96	2.07	2.10	1.60

"x" means undetectable

Table 1. Correction factor obtained from AFM and gel electrophoresis methods. (Adapted and modified from reference [13], with permission)

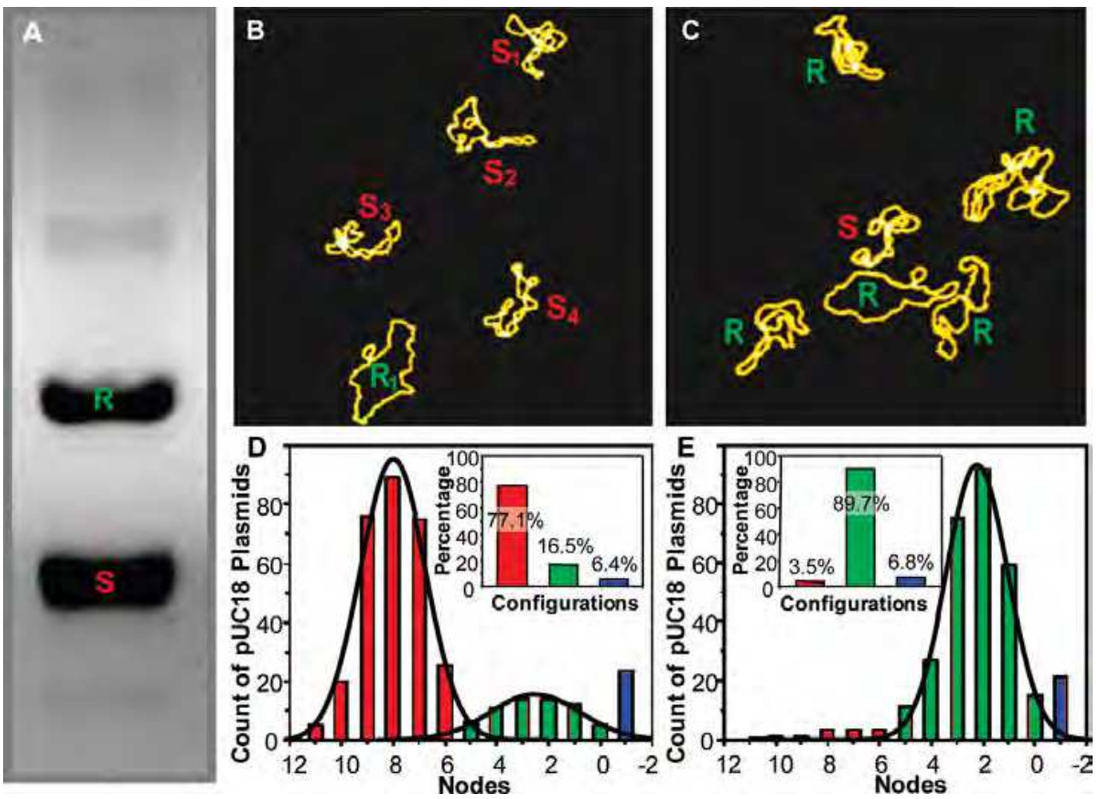

Fig. 8. (A) A photograph of the agarose gel showing separated supercoiled and relaxed pUC18 bands. AFM images of pUC18 DNAs that were extracted from agarose gel, (B) supercoiled band, and (C) relaxed band, as shown in part A. Scan size in both images is 1 × 1 μm^2. (D and E) Histograms showing the distributions of nodes of pUC18 plasmids counted from the AFM images such as those shown in parts B and C. The curves in the histogram show the Gaussian distribution fits. Inset figures show the histograms of the percentages of various conformations of pUC18 plasmids determined from the 6 nodes criterion. Color code: red, supercoiled DNA (S); green, relaxed circular plasmids (R); blue, linear DNA (L). The image was treated with flatten function in operation software (Veeco Inc.) to get rid of the background noise. (Adapted and modified from reference [13], with permission)

AFM images of these DNA obtained from supercoiled and relaxed DNA bands, respectively. Comparing Figure 8B with C, the conformations of DNA molecules are quite different. The DNA molecules obtained from the supercoiled band have significantly much more nodes (the number of visible crossover points in AFM images) than those from the relaxed band. Supercoiled and relaxed DNAs have obviously different node distributions as observed from this quantitative study as shown in Figure 8D and E. The plasmid molecules in the supercoiled band have about 6-11 nodes, while those in the relaxed band only have about 0-5 nodes [11]. These nodes count histograms were fitted with Gaussian distributions and 8.0±1.3 nodes (mean±standard deviation) was got for supercoiled DNA and 2.2±1.2 nodes for DNA in the relaxed band. According to these Gaussian distributions [11,13], the previous criterion [11] that we used to identify supercoiled and relaxed DNA is correct. The DNA molecules with more than 5 nodes can be considered as supercoiled, and those with 5 or less than 5 nodes are relaxed [11].

Moreover, according to this criterion, the distribution of percentages of various conformations of pUC18 plasmids was measured, and the results were shown as insets in Figure 8D and E. However, we found some deviations between AFM imaging and gel electrophoresis results. Only 77.1% of DNA extracted from the supercoiled band in the gel was actually supercoiled plasmids as shown in Figure 8B and D. Some relaxed molecules (16.5%) and even linear (6.4%) molecules were observed among the DNA extracted from the supercoiled band. These deviations may be caused by supercoiled DNA being damaged by the subsequent extraction processes and purification processes, and as a result degenerating into relaxed forms or linear forms. More significantly, from the AFM imaging results shown in Figure 8C and E, we can confirm small amounts (3.5%) of supercoiled molecules in our AFM images of the DNA extracted from the relaxed band. The number most likely represents the actual amount of supercoiled DNA in the relaxed band, since relaxed DNA cannot turn into supercoiled form automatically. The finding is direct evidence that gel electrophoresis may not be able to separate DNA entirely. Some supercoiled molecules will move to the "wrong" relaxed band, possibly due to molecular entanglement.

3.3 AFM can investigate the forces of the dynamic process of DNA

Besides AFM imaging, AFM force spectroscopy can also be used to analyze DNA quantitatively because it measures the relationship between molecular length and force, and has been used to examine the nanomechanics and mechanochemistry of DNA [36-38]. The technique has also proved unique in its ability to capture information about dynamic processes such as antigen-antibody complexes [39]. It can measure the length and tension of a single molecule with sub-nanometer (nM) and pico-newton (pN) resolution, respectively. A single DNA molecule was picked up by the AFM tip and stretched vertically in solution to determine it force-extension relationship [4].

Measurements of the force of DNA were carried out in solution, at room temperature, on an AFM instrument designed and equipped specifically for force spectroscopy measurements [40,41], as shown in Figure 9A. This instrument was built with a high accuracy piezoelectric *XYZ* stage equipped with three capacitive sensors, which offer an open-loop resolution of 0.1 nm in the *Z* axis and 1 nm in the *X* and *Y* axes. This instrument was also equipped with a commercial AFM head (Veeco Instruments Inc.). Untreated silicon nitride AFM cantilevers were used for picking up molecules and pulling measurements. The spring constant of each cantilever was measured in solution [19]. This measurement depended on attaching ssDNA molecules to the gold substrate and AFM tip by nonspecific adsorption, and this method has proved to be a simple, but effective method in previous DNA force spectroscopy studies [18,42]. For this methodology, the AFM tip picks up ssDNA fragments at random positions.

The force spectrograms, shown in Figure 9B, reveal two pronounced plateau features. The first plateau occurs at a force of 23 pN and overstretches the polynucleotide by about 80%. This lowforce plateau is very similar to the plateau theoretically predicted by Buhot and Halperin [43] based on their model of base-stacking interactions in poly(dA). The plateau likely represents the unwinding of the poly(dA) helix, and its force directly indicates the strength of base-stacking interactions among the adenines. The second plateau occurs at a force of about 113 pN and overstretches poly(dA) by an additional ~16%. We speculate that during this phase of base-unstacking, poly(dA) is still in the helical form, although this helix must be extended, and the high-force plateau represents the reorientation of bases, which is accompanied by the flip of the backbone bonds to new torsional states that increase the

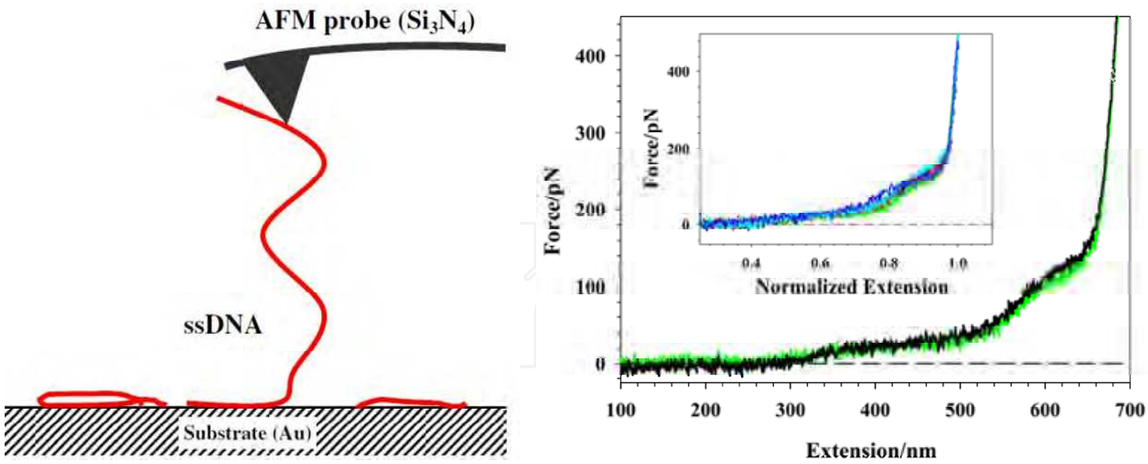

Fig. 9. (A). A schematic of single-molecule atomic force microscopy measurements of ssDNA molecules (the figure is not to scale). (B). typical force-extension measurement curves for poly(dA). The poly(dA) molecules were normalized corresponding to the longest molecule and the comparison between the stretching trace (green, online; gray, in print) and the relaxing trace (black). The inset plot shows the overlapping of six recorded force-extension curves of poly(dA) on a normalized extension basis. These recordings were obtained in different experiments on different poly(dA) molecules. (Adapted and modified from reference [35], with permission)

distance between the consecutive phosphates in a semidiscontinuous fashion. The reorientation of bases may, at higher forces, be also accompanied by a forced conformational transition in the deoxyribofuranose rings from their C3′ endo pucker (5.9 A° spacing between the neighboring phosphates) to a C2′ endo pucker (7A° spacing between the neighboring phosphates) [44,45]. Such a transition would produce an additional extension of the backbone chain up to 19%, which coincides with the width of the second plateau.

To research DNA methylation patterns, methylated single-stranded DNA molecules were linked to a glass substrate. An antibody was attached to the AFM tip that is specific towards 5-methylcytosine which has two free antigen-binding fragment arms (Figure 10a). Bringing the functionalized tip into contact with the DNA, two complexes formed between the two arms of the antibody and two 5-methylcytosines on the DNA.

Two characteristic force peaks was recorded by stretching the DNA-antibody complex, which they related to consecutive rupture events between the antibody arms and methylcytosines (Figure 10a) [46]. Since contacts between both the arms and various methylcytosines form randomly, the antibody arms may contact all possible pairs of methylated bases. The methylation patterns could then be obtained by analyzing the separations between force peaks. The first DNA oligomer examined by the group contained five equally spaced methylcytosines with three unmodified bases between neighbouring methylcytosines. It implies that there are four possible pairs in which the methylcytosines are separated by four nucleotide lengths: 3 pairs separated by 8 nucleotide lengths; 2 pairs that are separated by 12 nucleotide lengths and 1 pair separated by 16 nucleotide lengths (inset to Figure 10b). Hundreds of force spectroscopy measurements on this DNA sample

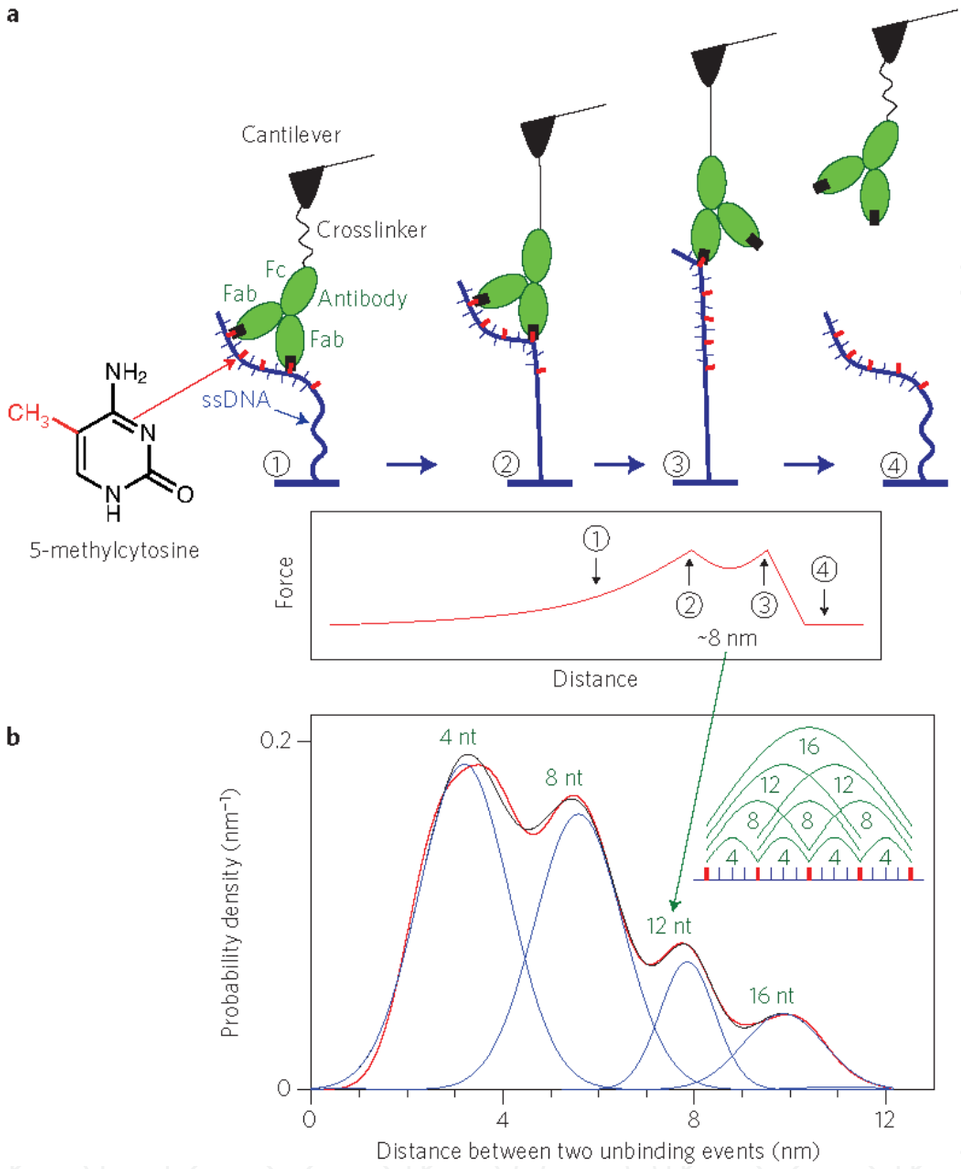

Fig. 10. A force-spectroscopy assay for detecting DNA methylation patterns. (A) Single-stranded DNA (ssDNA, blue lines) carrying methylated cytosines (red boxes; the chemical structure is shown in the inset) are coupled to a glass surface. The antibody (green) against 5-methylcytosine is tethered to the AFM cantilever tip, and the two arms bind to methylcytosines that are separated by a certain number of nucleotides (12 in this case). Panels 1–4 correspond to different stages during stretching of the antibody–DNA complex. These bonds break sequentially at stages 2 and 3, producing two characteristic force peaks in the force–extension curve (lower panel) that are separated by a distance equal to the spacing between two 5-methylcytidines in DNA. (B) Repeating this measurement numerous times produces a probability distribution of the distances between force peaks (red) that can be used to determine the methylation pattern. This distribution can be fitted by the sum of four Gaussian distributions (blue) of varying height that correspond to the different possible pairs of methylcytosines. (Adapted and modified from reference [46] with permission)

produced a relatively complex distribution of the spacing between two rupture events (Figure 10b). Notably, when the distribution was suitable for numerous Gaussian functions, four maxima at 4, 8, 12, and 16 nucleotides were identified. Furthermore, as expected, the relative amplitudes of these maxima were 4:3:2:1.

AFM can subject molecules to very high loads compared to other force measurement methods, such as optical or magnetic tweezers. The piezoelectric stages in AFMs can apply newtons of force, and the stiff cantilevers can detect large forces on the order of nanonewtons. Also, cantilevers and substrates can be functionalized with all types of chemistry, and that functionalization allows covalent bonds to form between the sample and the cantilever. On the contrary, optical and magnetic tweezers are limited by trap and magnetic field strength, respectively. The properties that make AFM so well suited for high force measurements are also what limit its function in the low force regime. The stiff cantilevers that can detect forces in the nanonewtons also exhibit much higher force noise, compared to the soft optical traps. Table 2 summarizes the force and spatial limits for these various force spectroscopy methods.

Method	Force range (N)	Spatial Resolution (m)	Adavantages
AFM	10^{-11}~10^{-7}	10^{-10}	High spatial resolution High applied forces
Magnetic Tweezers	10^{-14}~10^{-11}	10^{-8}	High force resolution Able to induce torque
Optical Tweezers	10^{-13}~10^{-10}	10^{-9}	High force resolution

Table 2. Force and spatial limits of common force spectroscopy methods. (Adapted and modified from reference [4], with permission)

4. Summary

AFM, which is normally used to gain qualitative results, can also be employed for quantitative research at a single-molecular level. By analyzing the numbers of DNA molecules with different topological configurations from AFM images, the distributions of DNA with different configurations can be identified directly. Based on this advantage, AFM imaging is ideal for quantifying DNA structure under a wide range of DNA amounts, concentrations and sizes that may not able to be handled by other methods. Atomic force microscopy is proven to be an accurate method in the identification and quantification of the plasmid with different topological structures, since these measurements are based on single-molecular observations. Thus, atomic force microscopy is a viable alternative to gel electrophoresis in the study of different DNA structures. The AFM force spectroscopy assay shows that AFM is also a very useful tool to analyze quantitatively the mechanical properties of individual DNA molecule. The structure of DNA, DNA-protein interaction and the dynamic processes that related to the mechanical properties can be measured accurately just by stretch single DNA between the substrate and the AFM tip.

5. Acknowledgements

We are grateful for the support of the National Natural Science Foundation of China (NSFC) to Y.J. uder Grant No. 21174029 and the startup fund from Southeast University to Y.J. under Grant No. 2009-81 and KJ2010479.

6. References

[1] Binnig, G., Quate, C. F. & Gerber, C. Atomic Force Microscope. *Physical Review Letters* 56, 930, doi:10.1103/PhysRevLett.56.930 (1986).

[2] Lyubchenko, Y. L. Preparation of DNA and nucleoprotein samples for AFM imaging. *Micron* 42, 196-206, doi:10.1016/j.micron.2010.08.011 (2011).

[3] Lauritsen, J. V. & Reichling, M. Atomic resolution non-contact atomic force microscopy of clean metal oxide surfaces. *J Phys Condens Matter* 22, 263001, doi:10.1088/0953-8984/22/26/263001 (2010).

[4] Rabbi, M. & Marszalek, P. E. Nanomechanics of nucleic acid structures investigated with AFM based force spectroscopy. *Ph.D. Dissertation of Duke University* (2010).

[5] Wang, H. *et al.* DNA bending and unbending by MutS govern mismatch recognition and specificity. *Proc Natl Acad Sci U S A* 100, 14822-14827, doi:10.1073/pnas.2433654100 (2003).

[6] Chen, L. W., Haushalter, K. A., Lieber, C. M. & Verdine, G. L. Direct visualization of a DNA glycosylase searching for damage. *Chemistry & Biology* 9, 345-350, doi:10.1016/s1074-5521(02)00120-5 (2002).

[7] Boichot, S. *et al.* Investigation of radiation damage in DNA by using atomic force microscopy. *Radiation Protection Dosimetry* 99, 143-145 (2002).

[8] Psonka, K., Brons, S., Heiss, M., Gudowska-Nowak, E. & Taucher-Scholz, G. Induction of DNA damage by heavy ions measured by atomic force microscopy. *Journal of Physics: Condensed Matter* 17, S1443-S1446, doi:10.1088/0953-8984/17/18/002 (2005).

[9] Lysetska, M. *et al.* UV light-damaged DNA and its interaction with human replication protein A: an atomic force microscopy study. *Nucleic Acids Res* 30, 2686-2691, doi:10.1093/nar/gkf378 (2002).

[10] Moreno-Herrero, F. *et al.* Mesoscale conformational changes in the DNA-repair complex Rad50/Mre11/Nbs1 upon binding DNA. *Nature* 437, 440-443, doi:10.1038/nature03927 (2005).

[11] Jiang, Y., Ke, C., Mieczkowski, P. A. & Marszalek, P. E. Detecting ultraviolet damage in single DNA molecules by atomic force microscopy. *Biophys J* 93, 1758-1767, doi:10.1529/biophysj.107.108209 (2007).

[12] Jiang, Y. *et al.* UVA generates pyrimidine dimers in DNA directly. *Biophys J* 96, 1151-1158, doi:10.1016/j.bpj.2008.10.030 (2009).

[13] Jiang, Y., Rabbi, M., Mieczkowski, P. A. & Marszalek, P. E. Separating DNA with different topologies by atomic force microscopy in comparison with gel electrophoresis. *J Phys Chem B* 114, 12162-12165, doi:10.1021/jp105603k (2010).

[14] Ke, C. *et al.* Nanoscale detection of ionizing radiation damage to DNA by atomic force microscopy. *Small* 4, 288-294, doi:10.1002/smll.200700527 (2008).

[15] Shlyakhtenko, L. S. *et al.* Silatrane-based surface chemistry for immobilization of DNA, protein-DNA complexes and other biological materials. *Ultramicroscopy* 97, 279-287, doi:10.1016/s0304-3991(03)00053-6 (2003).

[16] Lobachevsky, P. N., Karagiannis, T. C. & Martin, R. F. Plasmid DNA breakage by decay of DNA-associated auger electron emitters: Approaches to analysis of experimental data. *Radiation Research* 162, 84-95, doi:10.1667/RR3187 (2004).

[17] Sachs, R. K., Ponomarev, A. L., Hahnfeldt, P. & Hlatky, L. R. Locations of radiation-produced DNA double strand breaks along chromosomes: a stochastic cluster process formalism. *Mathematical Biosciences* 159, 165-187, doi:10.1016/s0025-5564(99)00019-x (1999).

[18] Rief, M., Clausen-Schaumann, H. & Gaub, H. E. Sequence-dependent mechanics of single DNA molecules. *Nature Structural Biology* 6, 346-349, doi:10.1038/7582 (1999).

[19] Florin, E. L. *et al.* SENSING SPECIFIC MOLECULAR-INTERACTIONS WITH THE ATOMIC-FORCE MICROSCOPE. *Biosensors & Bioelectronics* 10, 895-901, doi:10.1016/0956-5663(95)99227-c (1995).

[20] Cherny, D. I. & Jovin, T. M. Electron and scanning force microscopy studies of alterations in supercoiled DNA tertiary structure. *Journal of Molecular Biology* 313, 295-307, doi:10.1006/jmbi.2001.5031 (2001).

[21] Vologodskii, A. V. & Cozzarelli, N. R. CONFORMATIONAL AND THERMODYNAMIC PROPERTIES OF SUPERCOILED DNA. *Annual Review of Biophysics and Biomolecular Structure* 23, 609-643, doi:10.1146/annurev.bb.23.060194.003141 (1994).

[22] Folkard, M., Prise, K. M., Vojnovic, B., Brocklehurst, B. & Michael, B. D. Critical energies for ssb and dsb induction in plasmid DNA by vacuum-UV photons: an arrangement for irradiating dry or hydrated DNA with monochromatic photons. *International Journal of Radiation Biology* 76, 763-771, doi:10.1080/09553000050028913 (2000).

[23] Folkard, M., Prise, K. M., Turner, C. J. & Michael, B. D. The production of single strand and double strand breaks in DNA in aqueous solution by vacuum UV photons below 10 eV. *Radiation Protection Dosimetry* 99, 147-149 (2002).

[24] Chen, W. M., Blazek, E. R. & Rosenberg, I. THE RELAXATION OF SUPERCOILED DNA-MOLECULES AS A BIOPHYSICAL DOSIMETER FOR IONIZING-RADIATIONS - A FEASIBILITY STUDY. *Medical Physics* 22, 1369-1375, doi:10.1118/1.597420 (1995).

[25] Shlyakhtenko, L. S., Miloseska, L., Potaman, V. N., Sinden, R. R. & Lyubchenko, Y. L. Intersegmental interactions in supercoiled DNA: atomic force microscope study. *Ultramicroscopy* 97, 263-270, doi:10.1016/s0304-3991(03)00051-2 (2003).

[26] Bussiek, M., Mucke, N. & Langowski, J. Polylysine-coated mica can be used to observe systematic changes in the supercoiled DNA conformation by scanning force microscopy in solution. *Nucleic Acids Res* 31, doi:10.1093/nar/gng137 (2003).

[27] Murakami, M., Hirokawa, H. & Hayata, I. Analysis of radiation damage of DNA by atomic force microscopy in comparison with agarose gel electrophoresis studies. *Journal of Biochemical and Biophysical Methods* 44, 31-40, doi:10.1016/s0165-022x(00)00049-x (2000).

[28] Pang, D., Berman, B. L., Chasovskikh, S., Rodgers, J. E. & Dritschilo, A. Investigation of neutron-induced damage in DNA by atomic force microscopy: Experimental evidence of clustered DNA lesions. *Radiation Research* 150, 612-618, doi:10.2307/3579883 (1998).

[29] Pang, D., Rodgers, J. E., Berman, B. L., Chasovskikh, S. & Dritschilo, A. Spatial distribution of radiation-induced double-strand breaks in plasmid DNA as

resolved by atomic force microscopy. *Radiation Research* 164, 755-765, doi:10.1667/rr3425.1 (2005).
[30] Lyubchenko, Y. L. DNA structure and dynamics - An atomic force microscopy study. *Cell Biochemistry and Biophysics* 41, 75-98, doi:10.1385/cbb:41:1:075 (2004).
[31] Sperrazza, J. M., Register, J. C. & Griffith, J. ELECTRON-MICROSCOPY CAN BE USED TO MEASURE DNA SUPERTWISTING. *Gene* 31, 17-22, doi:10.1016/0378-1119(84)90190-2 (1984).
[32] Lushnikov, A. Y. *et al.* Interaction of the Zalpha domain of human ADAR1 with a negatively supercoiled plasmid visualized by atomic force microscopy. *Nucleic Acids Res* 32, 4704-4712, doi:10.1093/nar/gkh810 (2004).
[33] Lyubchenko, Y. L. & Shlyakhtenko, L. S. Visualization of supercoiled DNA with atomic force microscopy in situ. *Proc Natl Acad Sci U S A* 94, 496-501, doi:10.1073/pnas.94.2.496 (1997).
[34] SYBR Gold. *Clare Chenmical Research http://www.clarechemical.com/gold.htm*.
[35] Ke, C., Humeniuk, M., S-Gracz, H. & Marszalek, P. E. Direct Measurements of Base Stacking Interactions in DNA by Single-Molecule Atomic-Force Spectroscopy. *Physical Review Letters* 99, doi:10.1103/PhysRevLett.99.018302 (2007).
[36] Clausen-Schaumann, H., Seitz, M., Krautbauer, R. & Gaub, H. E. Force spectroscopy with single bio-molecules. *Current Opinion in Chemical Biology* 4, 524-530, doi:10.1016/s1367-5931(00)00126-5 (2000).
[37] Fisher, T. E., Marszalek, P. E. & Fernandez, J. M. Stretching single molecules into novel conformations using the atomic force microscope. *Nature Structural Biology* 7, 719-724, doi:10.1038/78936 (2000).
[38] Bustamante, C., Chemla, Y. R., Forde, N. R. & Izhaky, D. Mechanical processes in biochemistry. *Annual Review of Biochemistry* 73, 705-748, doi:10.1146/annurev.biochem.72.121801.161542 (2004).
[39] Kienberger, F., Ebner, A., Gruber, H. J. & Hinterdorfer, P. Molecular recognition imaging and force spectroscopy of single biomolecules. *Accounts of Chemical Research* 39, 29-36, doi:10.1021/ar050084m (2006).
[40] Lee, G. *et al.* Nanospring behaviour of ankyrin repeats. *Nature* 440, 246-249, doi:10.1038/nature04437 (2006).
[41] Marszalek, P. E., Oberhauser, A. F., Pang, Y. P. & Fernandez, J. M. Polysaccharide elasticity governed by chair-boat transitions of the glucopyranose ring. *Nature* 396, 661-664, doi:10.1038/25322 (1998).
[42] Clausen-Schaumann, H., Rief, M., Tolksdorf, C. & Gaub, H. E. Mechanical stability of single DNA molecules. *Biophys J* 78, 1997-2007, doi:10.1016/S0006-3495(00)76747-6 (2000).
[43] Buhot, A. & Halperin, A. Effects of stacking on the configurations and elasticity of single-stranded nucleic acids. *Physical Review E* 70, doi:10.1103/PhysRevE.70.020902 (2004).
[44] Olson, W. K. & Sussman, J. L. HOW FLEXIBLE IS THE FURANOSE RING .1. A COMPARISON OF EXPERIMENTAL AND THEORETICAL-STUDIES. *Journal of the American Chemical Society* 104, 270-278, doi:10.1021/ja00365a049 (1982).
[45] Daune, M. Molecular Biophyscis Structures in motion. *United States by Oxford University Press. New York*, 42-48 (1999).
[46] Zhu, R. *et al.* Nanomechanical recognition measurements of individual DNA molecules reveal epigenetic methylation patterns. *Nat Nanotechnol* 5, 788-791, doi:10.1038/nnano.2010.212 (2010).

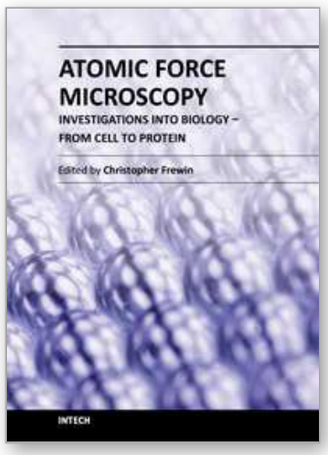

Atomic Force Microscopy Investigations into Biology - From Cell to Protein

Edited by Dr. Christopher Frewin

ISBN 978-953-51-0114-7
Hard cover, 354 pages
Publisher InTech
Published online 07, March, 2012
Published in print edition March, 2012

The atomic force microscope (AFM) has become one of the leading nanoscale measurement techniques for materials science since its creation in the 1980's, but has been gaining popularity in a seemingly unrelated field of science: biology. The AFM naturally lends itself to investigating the topological surfaces of biological objects, from whole cells to protein particulates, and can also be used to determine physical properties such as Young's modulus, stiffness, molecular bond strength, surface friction, and many more. One of the most important reasons for the rise of biological AFM is that you can measure materials within a physiologically relevant environment (i.e. liquids). This book is a collection of works beginning with an introduction to the AFM along with techniques and methods of sample preparation. Then the book displays current research covering subjects ranging from nano-particulates, proteins, DNA, viruses, cellular structures, and the characterization of living cells.

INTECH
open science | open minds

InTech Europe
University Campus STeP Ri
Slavka Krautzeka 83/A
51000 Rijeka, Croatia
Phone: +385 (51) 770 447
Fax: +385 (51) 686 166
www.intechopen.com

InTech China
Unit 405, Office Block, Hotel Equatorial Shanghai
No.65, Yan An Road (West), Shanghai, 200040, China
中国上海市延安西路65号上海国际贵都大饭店办公楼405单元
Phone: +86-21-62489820
Fax: +86-21-62489821

IntechOpen